DOI: 10.1534/genetics.104.036509

Infrequent Co-conversion of Markers Flanking a Meiotic Recombination Initiation Site in *Saccharomyces cerevisiae*

Lea Jessop,* Thorsten Allers† and Michael Lichten*,[1]

**Center for Cancer Research, National Cancer Institute, Bethesda, Maryland 20892 and †Institute of Genetics, University of Nottingham, Queen's Medical Centre, Nottingham NG7 2UH, United Kingdom*

Manuscript received September 18, 2004
Accepted for publication December 13, 2004

ABSTRACT

To study the mechanism of meiotic recombination in *Saccharomyces cerevisiae*, we examined recombination in an interval where the majority of events are initiated at a single hotspot for DNA double-strand breaks (DSBs), with little or no expected contribution by outside initiation events. This interval contained infrequently corrected palindromic markers 300 bp to the left and 600 bp to the right of the DSB hotspot. Conversion of single markers occurred frequently, while conversion of both markers occurred rarely, and many of the tetrads in which both markers converted were the products of multiple events. These data indicate that most meiotic recombination intermediates are asymmetrically positioned around the initiating DSB, with a short (<300 bp) tract of heteroduplex DNA (hDNA) to one side and hDNA on the other side frequently extending 600 bp or more. One consequence of this asymmetry is the preferential concentration of crossovers in the vicinity of the initiating DSB.

IN *Saccharomyces cerevisiae* and other organisms, recombination between homologous chromosomes is required to ensure proper segregation of chromosomes during meiosis (reviewed by Petronczki *et al.* 2003). Recombination is initiated by DNA double-strand breaks (DSBs) made by the meiosis-specific endonuclease Spo11 (Bergerat *et al.* 1997; Keeney *et al.* 1997). DSB sites tend to occur in clusters 100–200 nt wide (de Massy *et al.* 1995; Liu *et al.* 1995; Xu and Petes 1996); these clusters will be referred to as DSB hotspots. After DSB formation, break ends are resected to generate 3′ single-strand tails (Sun *et al.* 1991; Nag and Petes 1993). It has been proposed that these single strands invade homologous sequences and initiate DNA synthesis, ultimately forming joint molecules that contain two Holliday junctions flanking a tract of heteroduplex DNA (hDNA; Szostak *et al.* 1983). Evidence in support of this view comes from the isolation of double Holliday junction (dHJ) intermediates from meiotic yeast cells (Collins and Newlon 1994; Schwacha and Kleckner 1994) and the detection of hDNA in these intermediates (Allers and Lichten 2001b).

Gene conversion is a signal of the presence of hDNA. If unrepaired, a marker in asymmetric hDNA will segregate in a 5:3 or a 3:5 ratio of parental alleles among the eight strands of DNA present in the four haploid products of meiosis. These are postmeiotic segregation (PMS) events, so named because the two DNA strands that make up the hDNA segregate at the first mitotic division after meiosis (reviewed by Petes *et al.* 1991). If the mismatch is repaired, the marker will either be restored to parental (4:4) segregation or show full conversion (6:2 or 2:6) segregation. In this article, the term "gene conversion" encompasses both PMS and full conversion. Gene conversion is often, but not always, associated with an exchange of flanking markers. Gene conversions not associated with an exchange of flanking markers are referred to as noncrossovers (NCOs); events that involve an exchange of flanking markers are referred to as crossovers (COs).

The double-strand break repair (DSBR) model of Szostak *et al.* (1983), as modified by Sun *et al.* (1991), predicts that both NCOs and COs result from the resolution of a dHJ intermediate (Figure 1). COs are produced by cutting the two junctions in the opposite orientation, while cutting in the same orientation gives rise to NCOs. This model makes two significant predictions. First, hDNA will flank the DSB in both COs and NCOs, leading to frequent bidirectional conversion and hDNA present in two of the four meiotic products, which in *S. cerevisiae* are present as spores in a tetrad ascus. In one spore, hDNA will be present to the left of the DSB, and in the other spore, hDNA will be to the right. The second prediction is specific to CO products. The location of the Holliday junctions (HJs) in the dHJ intermediate as well as the direction of their resolution will dictate the point where unconverted markers appear to exchange linkage. If a single marker is included in hDNA, and if the two HJs are resolved in the opposite orientations, but without bias, then in half of the CO products the exchange point will be to the right of the

[1]*Corresponding author:* National Cancer Institute, Bldg. 37, Room 6124, 37 Convent Dr. MSC 4255, Bethesda, MD 20829-4255. E-mail: lichten@helix.nih.gov

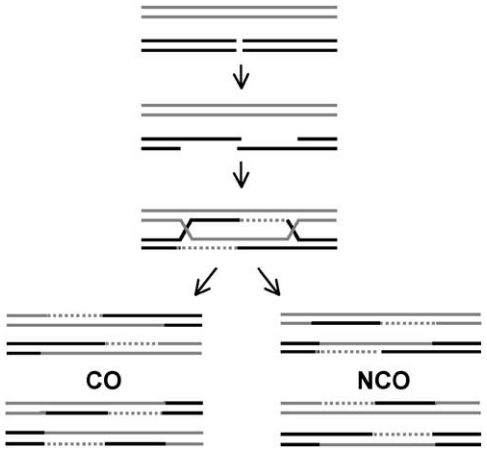

Figure 1.—DSBR model for meiotic recombination (Szostak *et al.* 1983; Sun *et al.* 1991). DSBs form and are resected to give 3′ single-strand tails. These tails invade homologous sequences and initiate DNA synthesis (broken lines) to form a dHJ intermediate. Both NCO and CO products are formed by junction cleavage; in every case, the two products contain hDNA on opposite sides of the DSB.

marker and in half it will be to the left (discussed in Gilbertson and Stahl 1996; for an illustration, see Figure 5). This can be determined only in tetrads where the relevant marker does not undergo full conversion (*i.e.*, shows PMS). Both predictions can be tested by examining patterns of gene conversion and crossing over in appropriately marked strains.

Several studies have examined the patterns of gene conversion in meiotic recombination. Schultes and Szostak (1990) used frequently corrected markers flanking the *ARG4* hotspot and found that, of events involving conversion of a marker 600 bp from the hotspot center, about two-thirds also showed conversion of a marker 300 bp on the other side. This result seemed to support the first prediction of the DSBR model—that hDNA flanks the DSB hotspot. However, the region used in this study contained a second DSB hotspot in the *DED81* promoter region, 2 kb away from the hotspot in the *ARG4* promoter (Sun *et al.* 1989). Events that initiated at the *DED81* DSB hotspot could have produced at least some of the observed co-convertants; others could have been the products of secondary events that have been suggested to be provoked by the action of mismatch repair on frequently corrected markers (Borts *et al.* 1990).

Gilbertson and Stahl (1996) and Porter *et al.* (1993) determined the location of hDNA in the products of meiotic recombination initiated at the *ARG4* and *HIS4* hotspots, respectively. These studies used palindromic markers, which frequently escape mismatch repair (Nag *et al.* 1989), thereby increasing the frequency of PMS and decreasing the likelihood of mismatch-repair-induced secondary events. Porter *et al.* (1993) rarely observed co-PMS for markers 900 bp to the left and 670 bp to the right of the *HIS4* DSB hotspot, with only 3% of events being bidirectional. Gilbertson and Stahl (1996) observed more frequent co-PMS for markers 130 bp to the left and 190 bp to the right of the *ARG4* DSB hotspot (55% of events that converted a marker in *ARG4* were bidirectional), but the location of hDNA in these products did not fit a central prediction of the DSBR model—that both recombinant products should contain hDNA. Instead, products showing PMS for both markers contained hDNA in only a single spore, and the majority of these products contained hDNA in a configuration most consistent with initiation at a site other than the *ARG4* DSB hotspot. Furthermore, the majority of PMS-associated crossovers mapped to the left of both markers in an interval that also contained the *DED81* DSB hotspot.

To detect hDNA and determine the timing of intermediate and recombinant product formation during meiosis, Allers and Lichten (2001a) used a physical assay to directly detect hDNA molecules. This assay examined ectopic recombination between dispersed reporter constructs inserted at *HIS4* and *LEU2*. Heteroduplex DNA associated with NCOs appeared at least 30 min before hDNA associated with COs. Mutants that accumulate dHJs, such as those lacking the meiosis-specific transcription factor Ntd80 or the polo-like kinase Cdc5, displayed a decrease in the formation of CO products but accumulated NCO products (Allers and Lichten 2001a; Clyne *et al.* 2003), indicating that formation of most NCO products does not depend upon dHJ resolution. These results led Allers and Lichten (2001a) to propose separate pathways for the formation of NCO and CO products. They suggested that NCOs arise by a synthesis-dependent strand annealing (SDSA) pathway (Paques and Haber 1999), where one DSB end invades the homolog and initiates DNA synthesis before being displaced and annealed with the other end of the DSB. They also suggested that the DSBR pathway, which generates dHJ intermediates, was involved primarily with CO formation. This accounts for the lack of NCO products with the hDNA pattern predicted by the DSBR model and the appearance of NCO products in the absence of dHJ resolution. NCO hDNA produced by single events in the SDSA pathway should be unidirectional and dHJ independent. The finding that mutants with defects in meiotic dHJ formation produce NCOs at normal frequencies (Börner *et al.* 2004) supports the suggestion that most NCOs are produced by SDSA.

Recently, Merker *et al.* (2003) examined conversion of markers <250 bp from each side of the *HIS4* DSB hotspot. In an effort to exclude events initiated at DSB sites other than the *HIS4* hotspot, their analysis focused on tetrads displaying gene conversion patterns that could have been produced by repair of a single DSB at the *HIS4* hotspot, using the DSBR mechanism in Figure 1. Of these, only 30% (16/56) were events where both markers displayed PMS. Many of these tetrads contained

TABLE 1

Diploid yeast strains

MJL2834	*HIS4* *leu2-R::URA3-tel-ARG4 MAT***a** *rad50-KI81::KanMX6*	
	his4::URA3-tel-ARG4 LEU2 *MAT*α *rad50-KI81::KanMX6*	
MJL2870	*HIS4* *leu2::ura3-EcPal+ 104-tel-ARG4 MAT***a**	
	his4::URA3-tel-arg4-EcPal+ 9 LEU2 *MAT*α	
MJL2902	*HIS4* *leu2::URA3-tel-ARG4 MAT***a**	
	his4::ura3-EcPal+ 104-tel-arg4-EcPal+ 9 LEU2 *MAT*α	
MJL2936	*his4::URA3-tel-ARG4* *PacI RHQ1-hphMX-FUS1 LEU2 MAT***a**	
	STE50-natMX-RRP7 his4::ura3-EcPal+ 104-tel-arg4-EcPal+ 9 *SphI* *leu2-R MAT*α	
MJL2957	*his4::URA3-tel-ARG4* *RHQ1-hphMX-FUS1 LEU2 MAT***a**	
	STE50-natMX-RRP7 his4::ura3-EcPal+ 104-tel-arg4-EcPal+ 9 *leu2-R MAT*α	
MJL2959	*his4-R::URA3-tel-ARG4* *PacI RHQ1-hphMX-FUS1 LEU2 MAT***a**	
	STE50-natMX-RRP7 his4::ura3-EcPal+ 104-tel-ARG4 *SphI* *leu2-R MAT*α	
MJL2961	*his4::URA3-tel-ARG4 MAT***a** *rad50-KI81::KanMX6*	
	*his4::URA3-tel-ARG4 MAT*α *rad50-KI81::KanMX6*	
MJL2976	*his4-R::URA3-tel-ARG4* *PacI RHQ1-hphMX-FUS1 LEU2 MAT***a**	
	STE50-natMX-RRP7 his4::URA3-tel-arg4-EcPal+ 9 *SphI* *leu2-R MAT*α	
MJL3010	*MAT***a** *rad50-KI81::KanMX6*	
	*MAT*α *rad50-KI81::KanMX6*	
MJL2960	*his4::URA3-tel-ARG4* *PacI RHQ1-hphMX-FUS1 LEU2 MAT***a** *rad50-KI81::kanMX6*	
	STE50-natMX-RRP7 his4::ura3-EcPal+ 104-tel-arg4-EcPal+ 9 *SphI* *leu2-R MAT*α *rad50-KI81::kanMX6*	

All strains are homozygous for *ura3*Δ*(hindIII-smaI) arg4*Δ*(eco47III-hpaI) lys2 ho::LYS2* (Allers and Lichten 2001a). *Pac*I/*Sph*I and *Eco*RI (*his4-R*) restriction site polymorphisms are described in materials and methods.

NCO recombinants, suggesting that, in addition to unidirectional NCO products that arise by the SDSA pathway, bidirectional NCO products may also arise via the DSBR pathway. Moreover, although Merker *et al.* (2003) did observe tetrads with patterns of bidirectional hDNA predicted by the DSBR model, their complete data set contains a greater number of tetrads that are most readily explained as being the products of multiple events.

Each of the genetic studies summarized here was done in a system where events producing recombinants could have initiated at more than one DSB hotspot, making it difficult to unambiguously identify the initiation site for a given conversion event. In some cases, many events were excluded in the effort to consider only events initiated by DSBs at a single hotspot. To reduce these complications, we examined recombination in an interval where most, if not all, events are initiated at a single DSB hotspot. To facilitate detection of hDNA in the products, we placed poorly corrected palindromic markers on each side of the DSB hotspot. Additional flanking markers allowed NCO and CO products to be distinguished as well as the position of the exchange point to be mapped. We examined both ectopic and allelic recombination events involving this interval. During ectopic recombination, flanking heterology prevents events initiated at outside sites from contributing to conversion of the palindromic markers. During allelic recombination, repression of DSBs at sites near the DSB hotspot present in the interval minimized contributions from other initiation sites. Data from these two configurations are in agreement, indicating that flanking heterologies present in the ectopic system do not substantially bias the outcome of recombination. We find that bidirectional conversion of markers flanking the DSB hotspot is infrequent and infer from these data that most meiotic recombination events involve at most a short tract of hDNA to one side of the DSB, while hDNA on the other side can frequently extend beyond 600 bp. This asymmetry, in combination with a possible resolution bias, results in a substantial concentration of crossovers in the vicinity of the initiating DSB.

MATERIALS AND METHODS

Strains and media: All diploid strains used in this study are SK1 derivatives (Kane and Roth 1974). Table 1 lists their genotypes. The recombination interval examined contains a 1.1-kb *Hin*dIII-*Sma*I *URA3* fragment and a 2.3-kb *Eco*47III-*Pst*I *ARG4* fragment inserted in a 64-bp *Cla*I-*Sal*I deletion of *HIS4* or at the *Eco*RV site of *LEU2*. The open reading frames (ORFs) of *URA3* and *ARG4* are arranged in a divergently transcribed configuration. The junction between the promoter regions of *URA3* and *ARG4* contains a 65-bp insert (5′-CAGCTGTCC CACACACACCACCCACACACACACCACACCCACACCACA

CCACACCCACTCTGCAG) derived from yeast teleomere sequences (White *et al.* 1993). The palindrome in *arg4-EcPal+9* is at +9 of the *ARG4* open reading frame (Allers and Lichten 2001a) and the palindrome in *ura3-EcPal+104* was inserted at an *Xba*I site created at +104 of the *URA3* open reading frame. The palindromes contain duplicated *Eco*RI sites, which allows physical detection. Strains used to study allelic recombination contained a hygromycin B resistance cassette (*hphMX*) inserted 5130 bp upstream of the start of the *HIS4* ORF and the nourseothricin resistance gene (*natMX*) inserted 3804 bp downstream of *HIS4* (Hoffmann *et al.* 2005). The *his4-R* restriction site mutant was constructed by filling in the *Eco*RI site 187 bp downstream of the *Cla*I site in *HIS4* to create an *Xmn*I site. The *Pac*I to *Sph*I restriction site was created by inserting an *Sph*I linker (GGCATGCC) into the *Pac*I site 223 bp upstream of the *HIS4* translation start. Details of strain construction will be supplied upon request.

Genetic procedures and media were as described (Allers and Lichten 2001a). Tetrads were dissected on solid media containing 2% peptone, 1% yeast extract, 4% glucose, 0.004% adenine, 2% agar, pH 5.5, and spores were germinated at 30°. Spores carrying *hphMX* or *natMX* were selected by replica plating spore colonies to YPD plates containing 300 μg/ml hygromycin B (Roche) or 100 μg/ml nourseothricin (Werner BioAgents).

CO determination: A subset of the ectopic COs generates the same marker configuration as an allelic CO in the interval between *HIS4* and *LEU2*. However, an ectopic CO leads to a deletion of the region between *HIS4* and *LEU2* in one of the products. Because this region contains no essential genes, haploid recombinants containing this deletion are viable. This region contains the *BIK1* and *FUS1* genes; *bik1*Δ *fus1*Δ strains efficiently mate with wild-type strains, but not with other *bik1*Δ *fus1*Δ strains (Trueheart *et al.* 1987). Spore colonies from strains MJL2902 and MJL2870 were replica plated to YPD plates and cross stamped with a lawn of either of two tester strains, H417 (*MAT***a** *ura3 ade1 trp5 lys2 met13-4 can1 cyh2 Δ[his4-LEU2]::URA3*) or H418 (same as H417, but *MAT*α), which are deleted for the region between *his4* and *LEU2*. After 4 hr on YPD, the plate was replica plated to minimal media plus 20 μg/ml histidine and 30 μg/ml lysine and incubated at 30° overnight. If the original spore colony was *bik1*Δ *fus1*Δ, it did not mate with the tester strain and so did not grow on selective media. If the spore colony was *BIK1 FUS1*, it did mate with the tester strain and the resulting diploid grew on selective media.

Pulsed-field gel electrophoresis: Samples for pulsed-field gel electrophoresis were prepared and run as previously described (Borde *et al.* 1999).

Random spore analysis: Separate patches of strains MJL2959 and MJL2976 were sporulated on plates containing 2% potassium acetate, 0.22% yeast extract, 0.05% glucose, and complete amino acid mixture (drop-out mix; Abdullah and Borts 2001) for ~24 hr. Ascus-cell mixtures were resuspended in 500 μl 1 M sorbitol, 10 mM EDTA, 50 mM KPO_4 (pH 7.5), 1% β-mercaptoethanol, and 1 mg/ml zymolyase 80T (ICN). Following incubation at 37° for 15 min, the spores were pelleted and resuspended in 1 ml 0.1% Tween-80. Spores were then sonicated until >90% were single spores as determined by microscopy. Appropriate dilutions were plated onto fresh YPD plates containing either 300 μg/ml hygromycin B or 100 μg/ml nourseothricin. After 2 days, at least 200 colonies were washed off the plates with sterile water and DNA was isolated from the pooled spore colonies as described in Goyon and Lichten (1993).

Molecular analysis: Approximately 2 μg of DNA was digested for 1 hr with 20 units *Eco*RI (New England Biolabs, Beverly, MA) and 10 units *Sph*I (Roche) in the recommended buffer for *Eco*RI (New England Biolabs) to determine the location of meiotic COs from MJL2959 and MJL2976. To map DSBs, DNA from meiotic cultures (Goyon and Lichten 1993) was digested with 40 units *Xho*I (Roche) or with 10 units of *Eco*RI (New England Biolabs) in the recommended buffer supplemented with 100 μM spermidine. Digests were displayed on agarose gels, gel blots were probed with a ^{32}P-labeled *ARG4* fragment (ARGD, +165–+1413, relative to the *ARG4* open reading frame), and band intensities were quantified as described (Allers and Lichten 2001b).

For fine-scale mapping of DSBs, 2 μg of DNA was digested with 4 units of *Ppu*MI (New England Biolabs) and 5 units of *Ban*II (New England Biolabs) in NEBuffer 4. DNA was electrophoresed through 5% polyacrylamide (37.5:1 acrylamide:bisacrylamide) in 0.5× Tris-borate-EDTA buffer (Sambrook and Russell 2001) and electroblotted to Zeta-Probe

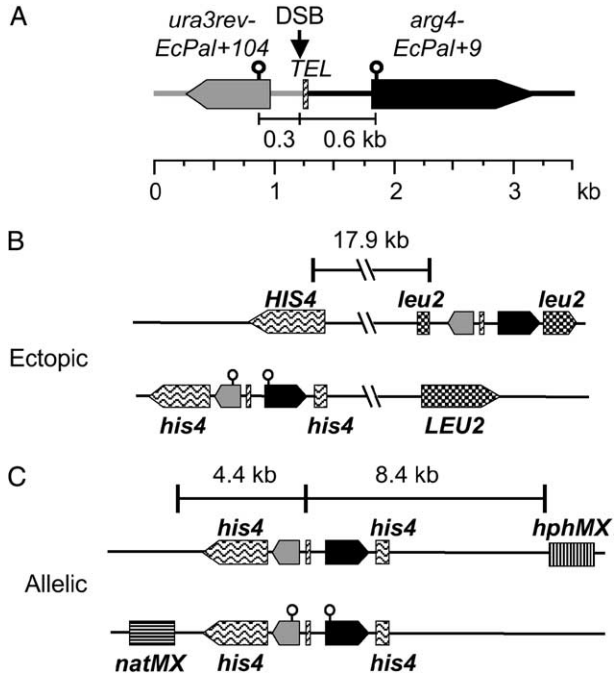

Figure 2.—The recombination assay systems used in this study. (A) The 3.5-kb *URA3-ARG4* insert. Coding sequences are represented by gray and black boxes and noncoding sequences are represented by gray and black lines. Inserted between *URA3* and *ARG4* is 65 bp of telomeric DNA (TEL, diagonally hatched box) that creates a strong meiotic DSB hotspot (see text) indicated by an arrow. Palindromic markers (lollipops) are inserted at +104 of the *URA3* open reading frame and at +9 of the *ARG4* open reading frame. These markers are ~200–340 and 520–660 bp from the center of the DSB hotspot, respectively. (B) Ectopic recombination system. The *URA3-ARG4* interval was inserted at *HIS4* (box with wavy hatching) on one copy of chromosome *III* and at *LEU2* (checkered box) on the homolog. The two insert sites at *HIS4* and *LEU2* are 17.9 kb apart in the SK1 strains used here. The marker configuration shown here is present in strain MJL2902, where the insert at *HIS4* contains *ura3-EcPal+104* and *arg4-EcPal+9*. In strain MJL2870, the insert at *LEU2* contains *arg4-EcPal+9* and the insert at *HIS4* contains *ura3-EcPal+104*. (C) Allelic recombination was examined between *URA3-ARG4* intervals inserted at *HIS4* on both copies of chromosome *III*. Homologs are distinguished by *natMX* (horizontally hatched box) or *hphMX* (vertically hatched box) insertions, ~4.4 and 8.4 kb from the center of the DSB hotspot, respectively.

GT membrane (Bio-Rad, Richmond, CA) in the same buffer. Prior to hybridization, DNA on the membrane was denatured by setting the membrane on filter paper saturated with 1.5 M NaCl and 0.5 M NaOH for 15 min; the blot was then probed as described (Liu *et al.* 1995) with a ^{32}P-labeled fragment −307–−80 nt relative to the *ARG4* open reading frame. Size markers on these gels contained digests of mitotic DNA from S1898 [*MAT*α *ura3*Δ*(hindIII-smaI) arg4*Δ*(eco47III-hpaI) lys2 ho::LYS2 rad50-KI81::KanMX6 cyh2-z leu2::URA3-tel-ARG4*].

RESULTS

Recombination in the *URA3-ARG4* interval is initiated from a single hotspot for DSBs: To determine the location of hDNA in the products of meiotic recombination, we modified the system used previously by Allers and Lichten (2001a) so that we could examine events initiated at a single DSB hotspot. This modified system consists of a 3.5-kb insert containing the *URA3* and *ARG4* genes with 65 bp of yeast telomere sequences inserted between *URA3* and *ARG4* to create a strong DSB hotspot (Figure 2A). This sequence induces a strong meiotic DSB hotspot when inserted elsewhere (White *et al.* 1993). The location and frequency of DSBs in the *URA3-ARG4* interval inserted at *HIS4* on both copies of chromosome *III* were mapped in a *rad50S* diploid (MJL2961, Table 1), where DSBs are neither processed nor repaired (Alani *et al.* 1990; Cao *et al.* 1990). Southern analysis reveals frequent DSBs in the vicinity of the telomeric sequences (Figure 3A). In a *rad50S* diploid heterozygous for inserts at *HIS4* and at *LEU2* (MJL2834; see below), DSBs occur in 16% of *his4::URA3-ARG4* inserts and 6% of *leu2::URA3-ARG4* inserts (data not shown). This disparity in DSB frequencies for inserts at *HIS4* and *LEU2* has been observed previously, although its cause has not been identified (Allers and Lichten 2001a). Fine-scale mapping using polyacrylamide gels reveals that the strong DSB is actually a cluster of at least four tightly spaced breaks, which occur over a region of ~130 bp immediately to the left of the telomeric sequences (Figure 3B). Similar DSB clusters have been observed at other meiotic DSB hotspots (de Massy *et al.* 1995; Liu *et al.* 1995; Xu and Petes 1996).

Co-conversion of markers flanking the DSB occurs rarely during ectopic recombination: To examine ectopic recombination, we inserted the *URA3-ARG4* recombination interval at *HIS4* on one copy of chromosome *III* and at *LEU2* on the homolog (Figure 2B). Because the interval is flanked by heterologous sequences, recombination events within the interval are most likely initiated by the internal hotspot with minimal or no contribution from outside events. To detect hDNA and score gene conversion associated with repair of the DSB, we inserted palindromes on both sides of the DSB hotspot at +104 of the *URA3* open reading frame (*ura3-EcPal+104*) and at +9 of the *ARG4* open reading frame (*arg4-EcPal+9*), as shown in Figure 2A. Because the DSB hotspot in this interval is spread over ~130 bp, *ura3-EcPal+104* is 200–340 bp from a DSB and *arg4-EcPal+9* is 520–660 bp from a DSB.

We examined ectopic recombination in two diploid strains that differ only in their marker configuration. MJL2902 contains both *ura3-EcPal+104* and *arg4-EcPal+9* inserted at *HIS4* (Figure 2B). In MJL2870, *ura3-EcPal+104* is present at *LEU2* and *arg4-EcPal+9* is at *HIS4*. Crossovers between the inserts occur in ~30% of tetrads in both strains (Table 2). In MJL2902 the gene conversion frequency (both PMS and full conversion events) of *ura3-EcPal+104* is 22%, somewhat greater than the 15% observed in MJL2870 (Table 2). The gene conversion frequency for *arg4-EcPal+9* is 14% in MJL2902 and 18% in MJL2870. In both strains, roughly half of the gene conversion events are associated with a CO (Table 2).

Although unidirectional conversion of these palindromes is frequent, co-conversion rarely occurs. In this work, we will refer to any tetrad with either PMS or full conversion of *ura3-EcPal+104* in one spore colony and either PMS or full conversion of *arg4-EcPal*+9 in any of the four spore colonies as having undergone co-conversion, without prejudgment as to whether these are the products of single or multiple events. Only 6% (50/840) of tetrads from MJL2902 and only 5% (37/744) of tetrads from MJL2870 show such co-conversion (Table 2). On the basis of the gene conversion frequencies of the two markers, co-conversion as a result of two independent events would be expected to occur in 3% of tetrads from both strains.

To further examine the likelihood that the majority of co-conversions result from multiple events, we examined tetrads that showed PMS for both palindromes. These tetrads are most informative, since they contain uncorrected hDNA on both sides of the DSB. From MJL2902 there were 23 such tetrads (for tetrad genotypes, see supplementary Appendix at http://genetics.org/supplemental/). Five of these tetrads cannot be the products of single events involving either the DSBR (Figure 1) or the SDSA pathways, because the markers converted in opposite directions—one of the two palindromic markers shows 3:5 segregation and the other shows 5:3 segregation. Since strain MJL2902 contains both mutant alleles on the same homolog, co-PMS events initiated by a single DSB should result in both markers segregating either 5:3 or 3:5. Three additional tetrads are most likely the result of multiple events, because more than two spores within the tetrad show gene conversion of the palindromic markers. Of the 15 remaining tetrads, 8 show a pattern of hDNA predicted by the DSBR model—one spore with hDNA on one side of the DSB and another spore with hDNA on the other side of the DSB. Six of these are CO associated. There are 7 other co-PMS tetrads, and these have hDNA in a single spore. Two of these show a *cis* PMS configuration, where parental contributions are on a single DNA strand on both sides of the DSB. This pattern of hDNA is also inconsistent with repair, by the mechanism shown in

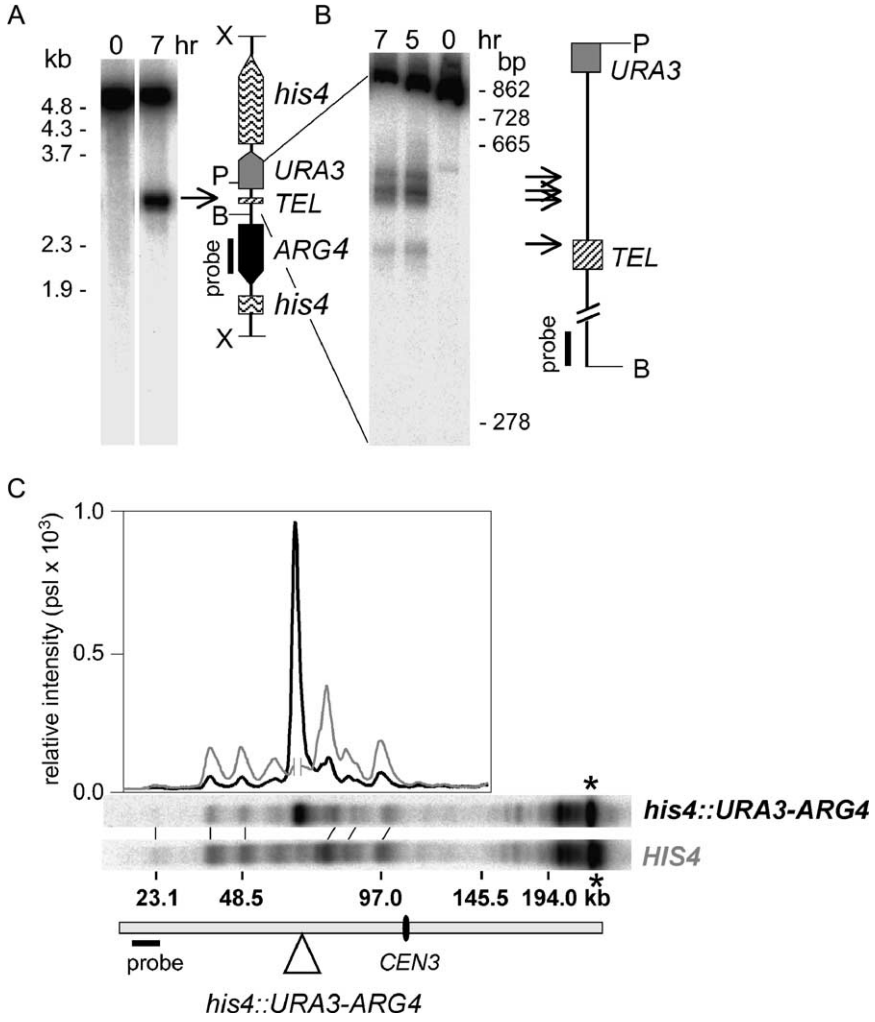

FIGURE 3.—DSBs in the *URA3-ARG4* interval. (A and B) Symbols are as in Figure 2. Southern blot of DNA isolated from a meiotic culture of MJL2961, a *rad50S* strain homozygous for the insertion at *HIS4*. (A) DNA from 0 and 7 hr after induction of meiosis was digested with *Xmn*I (X) and probed with *ARG4* sequences as described in MATERIALS AND METHODS. Size markers (lane not shown) are a *Bst*EII digest of bacteriophage λDNA. (B) For higher-resolution mapping of the DSB hotspot, DNA was digested with *Ppu*MI (P) and *Ban*II (B) and probed as described in MATERIALS AND METHODS. Arrows indicate the location of DSBs. Size markers (lane not shown) are *Mse*I (728 bp), *Msp*AI (665 bp), and *Ear*I (278 bp) digests of DNA from a mitotic culture of S1898 (see MATERIALS AND METHODS). The 862-bp size marker is a *Ban*II/*Ppu*MI digest of 0 hr DNA of MJL2961. (C) Pulsed-field gels of undigested DNA from meiotic cells, using electrophoresis conditions and a probe (*YCL075w*) to reveal DSBs on the left arm of chromosome *III*. (Top lane) Strain MJL2961; (bottom lane) strain MJL3010. Traces are of phosphorimager signals for the relevant portion of each lane (black line, MJL2961; gray line, MJL3010); peak intensities of the full-length chromosome *III* bands (marked with asterisks) are 2.1×10^3 psl and 1.9×10^3 psl for MJL2961 and MJL3010, respectively (psl are units that represent phosphor signal intensity). About 30% of chromosomes *III* suffer breaks in the left arm in both MJL2961 and MJL3010; in MJL2961, two-thirds of these breaks map to the *his4::URA3-ARG4* insert. The trace for MJL3010 is broken to account for the absence of an insert at *HIS4*. The position of the recombination interval relative to the centromere is indicated on the schematic; size markers (lane not shown) were a *Hin*dIII digest of bacteriophage λDNA and λDNA concatamers.

Figure 1, of a DSB from the central hotspot, and thus may be the product of multiple events. The remaining five tetrads contain hDNA in a single spore with parental contributions on opposite strands, *i.e.*, a *trans* configuration. Four of these are nonrecombinant for flanking markers and are thus compatible with topoisomerase-mediated unwinding of dHJ intermediates (GILBERTSON and STAHL 1996). Thus, of the 23 co-PMS tetrads from MJL2902, only 8 show the hDNA pattern predicted by the classic DSBR model (Figure 1). Similarly, 17 tetrads from MJL2870 show co-PMS. Six are most likely multiple events, as described for MJL2902. Five tetrads show the pattern of hDNA predicted by the DSBR model and three of these are CO associated.

Co-conversion is infrequent during allelic recombination: When sequences containing a strong DSB site are inserted at *HIS4*, they cause a reduction in DSBs at nearby sites (WU and LICHTEN 1995; FAN *et al.* 1997; T.-C. WU and M. LICHTEN, unpublished results). To examine the effect of the DSB hotspot within the *URA3-ARG4* interval on other DSB sites along the left arm of chromosome *III*, we performed pulsed-field gel analysis of meiotic DNA from MJL2961, which contains the *URA3-ARG4* interval at *HIS4* on both homologs, and from MJL3010, which does not contain the interval. DSBs at sites near the hotspot were reduced as much as fourfold relative to MJL3010 (Figure 3C), so that the majority of the DSBs in a 20-kb region centered around *his4::URA3-ARG4* occur at the hotspot. This strong repression of nearby breaks made it possible to examine recombination in strains containing allelic *his4::URA3-ARG4* inserts, with the expectation that most events were initiated by the DSB hotspot within the *URA3-ARG4* interval.

To distinguish COs from NCOs, strains in which one copy of chromosome *III* was marked with *natMX* (which confers nourseothricin resistance) and the homolog was marked with *hphMX* (which confers hygromycin B resistance) were constructed. The *natMX* and *hphMX* inserts are located ~4.4 kb to the left and 8.4 kb to the right

TABLE 2

Aberrant segregation and co-conversion

Strain	Tetrads	CO[a]	Allele	6:2	2:6	5:3	3:5	Other[b]	ABS (%)	CO/ABS (%)	PMS/ABS (%)	Co-conv[c]
MJL2902	840	32%	*ura3*	43	17	70	25	13	22	50	64	6%
		(270)	*arg4*	30	11	35	27	6	14	48	60	(50)
MJL2870	744	33%	*ura3*	18	11	33	41	5	15	47	71	5%
		(246)	*arg4*	35	9	34	31	11	18	53	60	(37)
MJL2936	388	54%	*ura3*	14	15	22	46	12	31	48	69	8%
		(210)	*arg4*	11	12	11	28	3	18	47	63	(31)
MJL2957	124	66%	*ura3*	8	5	6	11	2	29	62	62	7%
		(80)	*arg4*	3	2	8	8	1	19	71	78	(8)
Allelic[d]	512	57%	*ura3*	22	20	28	57	14	31	51	68	8%
		(290)	*arg4*	14	14	19	36	4	18	54	67	(39)
MJL2959	236	51%	*ura3*	7	15	12	28	5	28	57	67	
		(121)										

ura3, ura3-EcPal+104; arg4, arg4-EcPal+9; ABS, total aberrant segregation events/total tetrads; CO/ABS, fraction of tetrads showing aberrant segregation that is crossover associated; PMS/ABS, fraction of tetrads showing aberrant segregation where the palindromic marker shows PMS; co-conv, fraction of tetrads showing co-conversion.

[a] The interval for the ectopic crosses MJL2902 and MJL2870 is *URA3–ARG4*. For MJL2936, MJL2957, and MJL2959 the interval is *natMX–hphMX*. The number in parentheses is the total number of tetrads with a CO in the specified interval.

[b] 7:1, 1:7, 8:0, 0:8, and aberrant 4:4, 5:3, 3:5, 6:2, or 2:6 segregation patterns (see supplementary material at http://genetics.org/supplemental/ for details). Calculations of ABS frequencies assume that these were produced by two independent conversion events.

[c] The number in parentheses is the number of tetrads that showed co-conversion as defined in the text.

[d] Data from MJL2936 and MJL2957 were summed.

of the DSB hotspot. The chromosome marked by *natMX* carried *ura3-EcPal+104* and *arg4-EcPal+9* (Figure 2C). DSB mapping in a *rad50S* strain with this marker configuration (supplementary Figure 1 at http://www.genetics.org/supplemental/) confirmed that most breaks in an ~24-kb region occurred at the *URA3-ARG4* DSB hotspot. The next closest DSB site was at the *natMX* insert, 4.4 kb to the left of the *URA3-ARG4* DSB hotspot, with ~2.4% of chromosome *III*s broken; no DSBs were detected at the *hphMX* insertion or for at least 13 kb to the right of the *URA3-ARG4* DSB hotspot (supplementary Figure 1 at http://www.genetics.org/supplemental/). In addition, frequencies of DSBs at the *URA3-ARG4* DSB hotspot were not substantially altered either by the presence of the palindromic markers or by the presence of the drug-resistant insert markers (data not shown).

To examine patterns of allelic gene conversion, genetic data from two diploid strains, MJL2936 and MJL2957, were pooled. These two strains differ only by an *Sph*I restriction enzyme site polymorphism (RSP) upstream of *HIS4* that is absent in MJL2957. This RSP was used for physical mapping of exchanges (see below) and did not have a significant effect on conversion of *ura3-EcPal+104* or *arg4-EcPal+9* (Table 2; chi-square test). The pattern of allelic gene conversion of the palindromic markers in the *URA3-ARG4* interval at *HIS4* is similar to that seen for the ectopic recombination events: unidirectional conversion is frequent while co-conversion is not. Gene conversion of *ura3-EcPal+104* occurs in 31% of tetrads and 18% of tetrads have a gene conversion at *arg4-EcPal+104*. Roughly half of the gene conversion events are CO associated (Table 2). Co-conversion of both *ura3-EcPal+104* and *arg4-EcPal+9* occurs in 8% of tetrads; the frequency expected for two independent events is 6% of tetrads.

A total of 24 tetrads show co-PMS for the two palindromic markers, and 9 of these are clearly multiple events (for criteria, see discussion of MJL2902 above). Of the remaining 15 tetrads, only 6 have the pattern of hDNA predicted by the DSBR model, and 4 of these are CO associated. The 9 other co-PMS tetrads show PMS for both palindromic markers in a single spore; of these, only 2 contain hDNA in the *trans* NCO configuration that might be produced by topoisomerase-resolution of a dHJ intermediate. Thus, as was the case for ectopic recombination, the majority of allelic co-PMS products do not have structures predicted by the DSBR model (Figure 1).

Exchange is preferentially located near the DSB: In COs that are associated with PMS, as well as those that are not associated with conversion of the palindromic markers, the exchange point (the point where uncon-

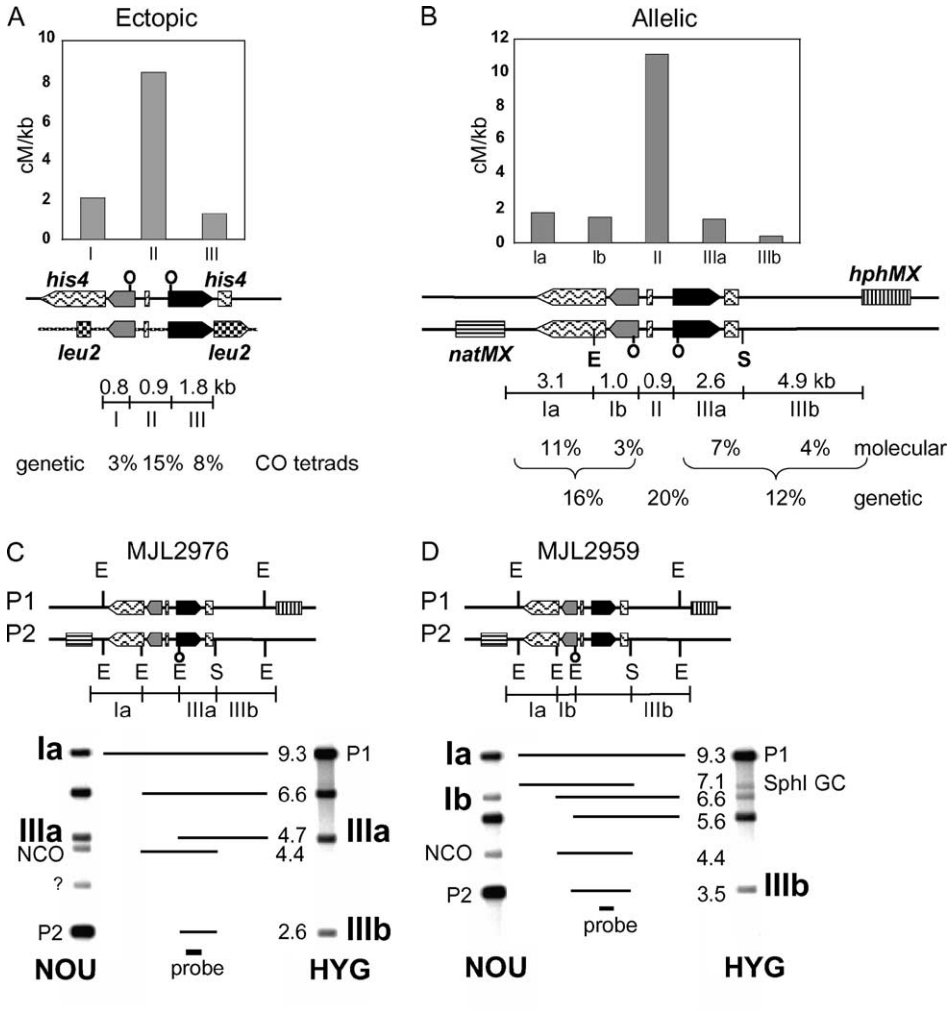

FIGURE 4.—Position of the exchange point among CO products. Symbols are as in Figure 2. (A) In the ectopic recombination system, the exchange point can be located in one of three intervals defined by flanking heterology (wavy and checkered boxes) and by the two palindromic markers (lollipops). The size (in kilobases) and frequency of exchanges mapped to the interval (percentage of crossover tetrads) are given below the schematic; crossover intensity (centimorgans per kilobase) in each interval is given in the bar graph above. The average crossover intensity for chromosome *III* is 0.48 cM/kb (CHERRY *et al.* 2002). Values reflect combined data from MJL2902 and MJL2870. The frequency of exchange (crossover tetrads/total tetrads) in intervals I, II, and III is 3%, 14%, and 8% for MJL2902 and 3%, 17%, and 7% for MJL2870. An additional 3% of combined tetrads had an exchange that could have occurred in either interval I or interval II; an additional 4% of combined tetrads had an exchange that could have occurred in either interval II or interval III. (B) In the allelic recombination system, intervals I and III are subdivided by restriction enzyme site polymorphisms for *Eco*RI (E) and *Sph*I (S) as described in the text. "Genetic" refers to the frequency of tetrads with exchange that mapped to intervals I, II, and III; values reflect combined data from MJL2936 and MJL2957. An additional 5% of tetrads had an exchange that could have occurred in either interval I or interval II, and an additional 3% of tetrads had an exchange that could have occurred in either interval II or interval III. "Molecular" refers to the frequency of tetrads expected to have an exchange in the subintervals Ia, Ib, IIIa, and IIIb, as calculated from physical analysis of DNA from random spores (see text). The bar graph shows the crossover intensity (centimorgans per kilobase) in each of the five intervals. Values for intervals Ia, Ib, IIIa, and IIIb were calculated from molecular data and, for interval II, from tetrad analysis. (C) Physical analysis of DNA isolated from either nourseothricin-resistant (NOU) or hygromycin-B-resistant (HYG) spore colonies of MJL2976. The schematic represents the marker configuration in this strain: one of the homologs is marked by *natMX* (horizontally hatched rectangle) and contains *arg4-EcPal+ 9* at *HIS4*. The other homolog is marked by *hphMX* (vertically hatched rectangle). Intervals Ib and II cannot be distinguished because *ura3-EcPal+ 104* is absent. DNA was isolated from a pool of at least 200 colonies, digested with *Eco*RI (E) and *Sph*I (S), and fragments were probed for *ARG4* sequences downstream of the palindromic marker. From nourseothricin-resistant spore colonies of MJL2976, the 9.3-kb fragment results from COs with the exchange point in interval Ia; the 6.6-kb fragment is from an exchange in interval Ib, II, or gene conversion of *arg4-EcPal+ 9* associated with an exchange in interval IIIa; the 4.7-kb fragment results from COs with an exchange point in interval IIIa; the 4.4-kb band is the NCO product; and the 2.6-kb band is the parental fragment. From the hygromycin-B-resistant colonies, the 9.3-kb band is the parental fragment; the 6.6-kb band results from exchanges in interval Ib, II, or gene conversion of *arg4-EcPal+ 9* associated with an exchange in interval IIIa; the 4.7-kb band is from COs with exchange in interval IIIa or gene conversion of the *Sph*I site; and the 2.6-kb band is the result of COs with exchange in interval IIIb. The source of the contaminant (?) in the NOU lane is unknown. (D) Physical analysis of DNA isolated from either nourseothricin-resistant or hygromycin-B-resistant spore colonies of MJL2959, analyzed as in C. This strain contains *ura3-EcPal+ 104* at *HIS4* on the homolog marked with *natMX*. Intervals II and IIIa cannot be distinguished because *arg4-EcPal+ 9* is absent. From nourseothricin-resistant spore colonies, the 9.3-kb fragment results from exchanges in interval Ia; the 6.6-kb band is the result of exchanges in interval Ib; the 5.6-kb band results from exchanges in II, IIIa, or gene conversion of the *Sph*I site; the 4.4-kb band is the NCO product; and the 2.6-kb band is the parental fragment. From the hygromycin-B-resistant colonies the 9.3-kb band is the parental fragment; the 7.1-kb fragment results from gene conversion of the *Sph*I site; the 6.6-kb band results from gene conversion of *ura3-EcPal+ 104* associated with exchange in intervals IIIa and II or from a CO in interval Ib; the 5.6-kb band results from gene conversion of *ura3-EcPal+ 104* exchanges in intervals II or IIIa; and the 3.5-kb band results from exchanges in interval IIIb.

TABLE 3

Crossover distributions

Strain	Conversion type	Crossover interval				
		I	I or II	II	II or III	III
MJL2902	None	12		73		47
	Full *ura3*		32			2
	PMS *ura3*	4	1	21		8
	Full *arg4*	0			12	
	PMS *arg4*	2		13		3
	Co-conversion	10	4	10	4	7
	Total	28	37	117	16	67
MJL2870	None	15		88		36
	Full *ura3*		15			0
	PMS *ura3*	6		12		2
	Full *arg4*	0			20	
	PMS *arg4*	1		15		10
	Co-conversion	3	4	7	5	4
	Total	25	19	122	25	52
Allelic	None	55		63		41
	Full URA3		20			0
	PMS URA3	18	4	27		5
	Full *arg4*	1			10	
	PMS *arg4*	3		8		6
	Co-conversion	6	3	4	6	9
	Total	81	27	102	16	61

Intervals I, II, and III are illustrated in Figure 4. Allelic data are pooled from MJL2936 and MJL2957, as in Table 2. In tetrads with full conversion or aberrant 4:4 segregation of *ura3-EcPal+ 104*, COs in intervals I and II cannot be distinguished; in tetrads with full conversion or aberrant 4:4 segregation of *arg4-EcPal+ 9*, COs in intervals II and III cannot be distinguished.

verted markers appear to exchange linkage) can be mapped to specific intervals on the basis of the pattern of exchange of flanking markers relative to palindromic markers. There are three genetic intervals in the ectopic recombination system: interval I is to the left of *ura3-EcPal+ 104*, interval II is between *ura3-EcPal+ 104* and *arg4-EcPal+ 9*, and interval III is to the right of *arg4-EcPal+ 9* (Figure 4A). The exchange point in ectopic COs could be mapped to one of these three intervals in 212 tetrads from MJL2902 and in 199 tetrads from MJL2870 (Table 3 and Figure 4A). COs associated with a full conversion of either of the palindromes cannot be mapped to a single interval and so were not considered in this analysis. There are roughly twofold more exchanges in interval III than in interval I. The 0.9-kb interval II, which contains the DSB hotspot, contains the majority (~60%) of the exchanges that can be mapped to one of the three intervals in the 3.5-kb *URA3-ARG4* region. The crossover density (crossovers per unit of physical distance) in this central interval is four to six times greater than that in the other two intervals (Figure 4A).

A substantial fraction of ectopic crossovers occurred without associated gene conversion. About one-third of total ectopic crossovers (161/508) have an exchange point in interval II without associated gene conversion, and 22% (110/508) of total ectopic crossovers have an exchange point in intervals I or III without associated gene conversion. Possible origins for the crossovers where the exchange point is separated from the most likely initiation (DSB) site by an unconverted marker will be discussed below.

The flanking intervals in the allelic recombination system are much larger than those in the ectopic system (Figure 4, A and B). Interval I is between *natMX* and *ura3-EcPal+ 104* (4.1 kb) and interval III is between *arg4-EcPal+ 9* and *hphMX* (7.5 kb). To allow a more direct comparison of exchange distributions, we used RSPs flanking the *URA3-ARG4* interval to subdivide intervals I and III. Interval Ia lies between *natMX* and the *Eco*RI RSP (3.1 kb). Interval Ib is from the *Eco*RI RSP to *ura3-EcPal+ 104* (1.0 kb). Similarly, intervals IIIa and IIIb are from *arg4-EcPal+ 9* to the *Sph*I RSP (2.6 kb) and the *Sph*I RSP to *hphMX* (4.9 kb), respectively (Figure 4B). This creates an *Eco*RI-*URA3-ARG4-Sph*I region (intervals Ib, II, and IIIa in Figure 4B) that more closely approximates the *URA3-ARG4* region of homology examined in ectopic crosses. To show that the two RSPs have no effect on conversion of the palindromic markers, we analyzed tetrads from MJL2957 and MJL2959, two strains related to MJL2936. MJL2957 lacks the *Sph*I RSP present in MJL2936 and these two strains show similar gene conversion frequencies (Table 2). MJL2959, which carries only *ura3-EcPal+ 104*, is heterozygous for the *Eco*RI site in *HIS4*. This strain and MJL2936 show similar gene conversion frequencies for the palindromic marker (Table 2). Thus, neither of the RSPs markedly affects gene conversion of *ura3-EcPal+ 104* or *arg4-EcPal+ 9*.

The distribution of exchange in intervals Ia, Ib, IIIa, and IIIb was determined by molecular analysis of DNA from the meiotic products of MJL2959 and MJL2976, using the flanking *Eco*RI and *Sph*I RSPs in combination with the *Eco*RI sites introduced by the *ura3-EcPal+ 104* and *arg4-EcPal+ 9* alleles. DNA was isolated from pools of at least 200 spore colonies that were selected to be resistant to either nourseothricin or hygromycin B. The DNA was digested with *Eco*RI and *Sph*I, and Southern blots of the resulting fragments were probed with *ARG4* sequences downstream of the palindromic marker (Figure 4, C and D). By this method, we estimate that 11% and 3% of tetrads display exchange in intervals Ia and Ib, respectively. Similarly, we estimate that 7% of tetrads display exchange in interval IIIa and 4% in interval IIIb. These values are in agreement with the frequencies of exchange in interval I (16%) and interval III (12%) determined by genetic analysis (Figure 4B). The distribution of exchange in the three central intervals (Ib, II, and IIIa) is similar to that seen in the ectopic configuration (compare Figure 4, A and B). In particular, 20% of tetrads

(102/512) contain crossovers where the exchange maps to the central interval II (Table 3), an exchange density that is more than fivefold greater than the exchange density seen in flanking intervals (Figure 4B). The similar exchange-density maps seen in both ectopic and allelic configurations indicates that the preference for DSB-proximal exchange (COs where the exchange point is between the two palindromic markers) is not due to a restriction of branch migration imposed by the extensive flanking heterology present during the ectopic recombination.

The above conclusion assumes that gene conversion of the RSPs or co-conversion of a RSP with a palindromic marker did not appreciably contribute to recombinants detected by the molecular analysis. We believe that both types of events are rare. For MJL2959, nourseothricin-resistant spore colonies that co-convert the *Eco*RI RSP and *ura3-EcPal+104* will yield a 7.1-kb fragment in the molecular analysis shown in Figure 4D. This band is not detected (<0.3% of total DNA). The same 7.1-kb band among hygromycin-B-resistant colonies could be the product of either a full gene conversion event in which the *hphMX* marked chromosome gains an *Sph*I restriction site or an exchange in interval IIIa or II that is associated with co-conversion of *ura3-EcPal+104* and the *Eco*RI RSP. This product is present at a level corresponding to ~1% of tetrads (Figure 4D). If this is taken as the maximum frequency for either gene conversion of the *Sph*I RSP or co-conversion of *ura3-EcPal+104* and the *Eco*RI RSP, the results presented in Figure 4B are not substantially altered.

We note that, in the allelic configuration, 11% of COs are estimated to occur in interval Ia and 4% in interval IIIb (Figure 4B). Moreover, one-third (96/290) of COs in the *natMX-hphMX* region show exchange in intervals I and III without associated gene conversion of the two palindromic markers. Possible origins for these crossovers will be discussed below.

Contribution of different dHJ resolution modes to exchange point location: According to the DSBR model (Figure 1), the exchange point in CO products should always be located at the end of a hDNA tract that starts at the DSB itself. In the case of unidirectional conversions, which compose the majority of events that we observed, one HJ should be located DSB proximal to the converted marker while the other should be DSB distal to the converted marker on the side of the converted marker opposite from the DSB (Figure 5). If we consider an intermediate in which only the *arg4-EcPal+9* marker is located in hDNA, COs produced by cutting the stands opposite the newly synthesized DNA (type 1 resolution in Figure 5) results in the exchange point being located DSB distal, to the right of *arg4-EcPal+9*. If the junctions are resolved by cutting the strands containing the newly synthesized DNA (type 2 resolution in Figure 5), the exchange point will be located proximal to the DSB, to the left of *arg4-EcPal+9*. Similarly, for CO-associated gene conversion of *ura3-EcPal+104*, the exchange point will be either distal (to the left of the marker, type I resolution) or DSB proximal (to the right of the marker, type 2 resolution). If the two types of resolution occur at equal frequencies, then an equal number of DSB-proximal and DSB-distal COs are expected to accompany PMS for a marker. We examined tetrads with CO-associated PMS of either *ura3-EcPal+104* or *arg4-EcPal+9* and determined the position of the exchange point relative to the unconverted markers. In both ectopic and allelic crosses, PMS-associated DSB-proximal COs (type 2 resolution) were present in excess of DSB-distal COs (type 1 resolution), but only in one case (MJL2902) did proximal *vs.* distal values differ significantly from equivalence (Fisher's exact test, $P < 0.005$). However, when our data are taken in aggregate, 68% of COs

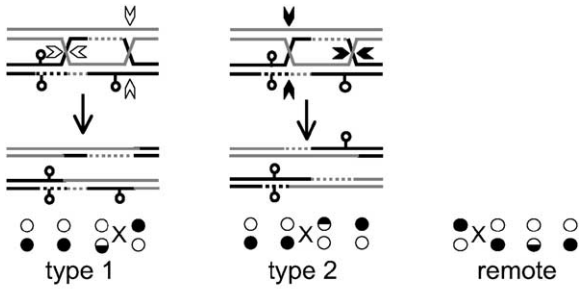

	PMS only at	Crossover type 1	type 2	remote
MJL2902	*ura3*	4	21	8
(ectopic)	*arg4*	3	13	2
	total	**7**	**34**	**10**
MJL2870	*ura3*	6	12	2
(ectopic)	*arg4*	10	15	1
	total	**16**	**27**	**3**
Allelic	*ura3*	18	27	5
	arg4	6	8	3
	total	**24**	**35**	**8**

Figure 5.—Resolution of the dHJ intermediate. The intermediate diagrammed here is for the marker configuration in MJL2902, or the allelic cross, and can be resolved in two ways to give rise to CO-associated gene conversion of *arg4-EcPal+9*. Type 1 resolution (open arrowheads) cuts the HJ on the continuous stands that do not contain newly synthesized DNA and leads to a DSB-distal exchange to the right of *arg4-EcPal+9*. Type 2 resolution (solid arrowheads) cuts the HJs on the strands containing newly synthesized DNA and their equivalent strands on the other duplex leading to a DSB-proximal exchange to the left of *arg4-EcPal+9*. "Remote" refers to tetrads where an unconverted palindromic maker separates the crossover from the palindromic marker in hDNA. The table lists the number of tetrads with unidirectional PMS conversion for either *ura3-EcPal+104* or *arg4-EcPal+9* with type 1, type 2, or remote resolution. The solid and open circles represent the genotype of the tetrad colonies where the parental configuration was ○○○○/●●●●. Circles that are half-white represent PMS. X marks the exchange point.

(96/142) display type 2 *vs.* type 1 resolution, a value significantly different from equivalence (Fisher's exact test: $P < 0.005$) and similar to that calculated for gene conversion of markers in the *HIS4* gene itself (67%; Foss *et al.* 1999).

We also observed tetrads where the exchange point is separated from the converted marker by an unconverted marker, but still involves the gene-converted chromatid. For example, two tetrads from MJL2902 show PMS for *arg4-EcPal+9*, with the exchange point located downstream of the unconverted *ura3-EcPal+104* in interval I (Figure 5). Possible origins for this class of products will be discussed below. Its frequency (~4% of conversion tetrads) is not significantly greater than that expected for independent events (~3% on the basis of crossover frequencies in nonconversion tetrads; $P = 0.15$, one-tailed Fisher's exact test).

DISCUSSION

Co-conversion of markers flanking the DSB hotspot is infrequent: We examined the pattern of hDNA resulting from meiotic recombination initiated at a single DSB hotspot with little or no expected contribution from initiation events occurring outside the interval. We find that bidirectional conversion occurs infrequently when the markers examined are ~300 and 600 bp from the DSB hotspot. In both allelic and ectopic recombination, the fraction of tetrads displaying simultaneous conversion of *ura3-EcPal+104* and *arg4-EcPal+9* was only slightly greater than that predicted for independent events (allelic, 8% *vs.* 6%; ectopic, 6% *vs.* 3%). Moreover, patterns of hDNA in tetrads with PMS for both markers infrequently corresponded to those predicted by the DSBR model (13/40 and 6/24 for ectopic and allelic configurations, respectively) while a similar fraction (14/40 and 9/24) were unambiguously the product of multiple events. We therefore believe it likely that, at this recombination hotspot, most co-conversion tetrads result from independent events rather than from true bidirectional conversion and that the majority of conversion events (at least 80% and possibly >90%) initiated at this DSB hotspot are unidirectional, involving gene conversion of only one of the two markers that flank the initiating DSB.

In the simplest terms, this finding would imply that heteroduplex DNA formation is similarly unidirectional. Other interpretations that involve bidirectional heteroduplex formation coupled with near-obligate restoration of markers on one side of the break by a mismatch correction system that is *MSH2/MLH1* independent and that corrects palindrome mismatches at high efficiency (Foss *et al.* 1999; Hoffmann *et al.* 2005) have been proposed. While such mechanisms are not excluded by current data, we will assume in the remainder of this discussion that all molecules with a palindrome in hDNA are treated equally with regard to likelihood and direction of mismatch correction and that gene conversion patterns for such markers accurately reflect underlying patterns of hDNA.

Other studies: Although others have examined the pattern of gene conversion resulting from meiotic recombination, each of those studies used a system in which more than one initiation site was present. Both Schultes and Szostak (1990) and Gilbertson and Stahl (1996) examined gene conversion of markers flanking the *ARG4* DSB hotspot, and both obtained evidence for frequent co-conversion. While this has been interpreted as indicating that many of the events that initiated at the *ARG4* DSB hotspot were bidirectional, the possibility that some co-conversion events were initiated at a second DSB hotspot, located ~2 kb away in the *DED81* promoter (Sun *et al.* 1989), cannot be eliminated. Furthermore, a substantial fraction of the co-conversions that Gilbertson and Stahl (1996) detected have marker configurations consistent with derivation from events that initiated at *DED81* and proceeded unidirectionally through the two markers. Gilbertson and Stahl (1996) used poorly corrected palindromic markers and thus were able to determine the pattern of hDNA present in the recombination products of a subset of tetrads. Only a minor fraction of the co-PMS tetrads that they observed had the pattern of hDNA predicted for events initiated at the *ARG4* DSB hotspot and proceeded as predicted by the DSBR model in Figure 1. That is, only 4/108 co-PMS tetrads showed PMS for a marker on one side of the *ARG4* DSB in one spore and PMS for the marker on the other side of the DSB in a different spore.

The pattern of co-conversion from recombination events initiated at the *HIS4* DSB hotspot has also been examined. Porter *et al.* (1993) found that only a small fraction of events initiated by breaks at this hotspot resulted in co-conversion of markers 670 bp to the right and 900 bp to the left of the hotspot. We find that when hDNA to one side of the DSB is >600 bp, hDNA on the other side does not extend beyond 300 bp. Recently, Merker *et al.* (2003) examined co-conversion of markers closer to the *HIS4* DSB hotspot—140 bp to the left and 240 bp to the right. They also observed frequent unidirectional conversion and concluded that initial strand invasion was shorter than the length of resection. They observed a greater frequency of bidirectional conversion than we did, although some of these events could have been produced either by two independent initiations or by events initiated elsewhere. In their study, 30% (16/56) of tetrads classified as products of single events showed a marker pattern consistent with the distribution of hDNA predicted by the DSBR model. Since the palindromic markers used by Merker *et al.* (2003) are located closer to the DSB hotspot than the markers used in our study, their detection of more frequent co-conversion would indicate that the initial inva-

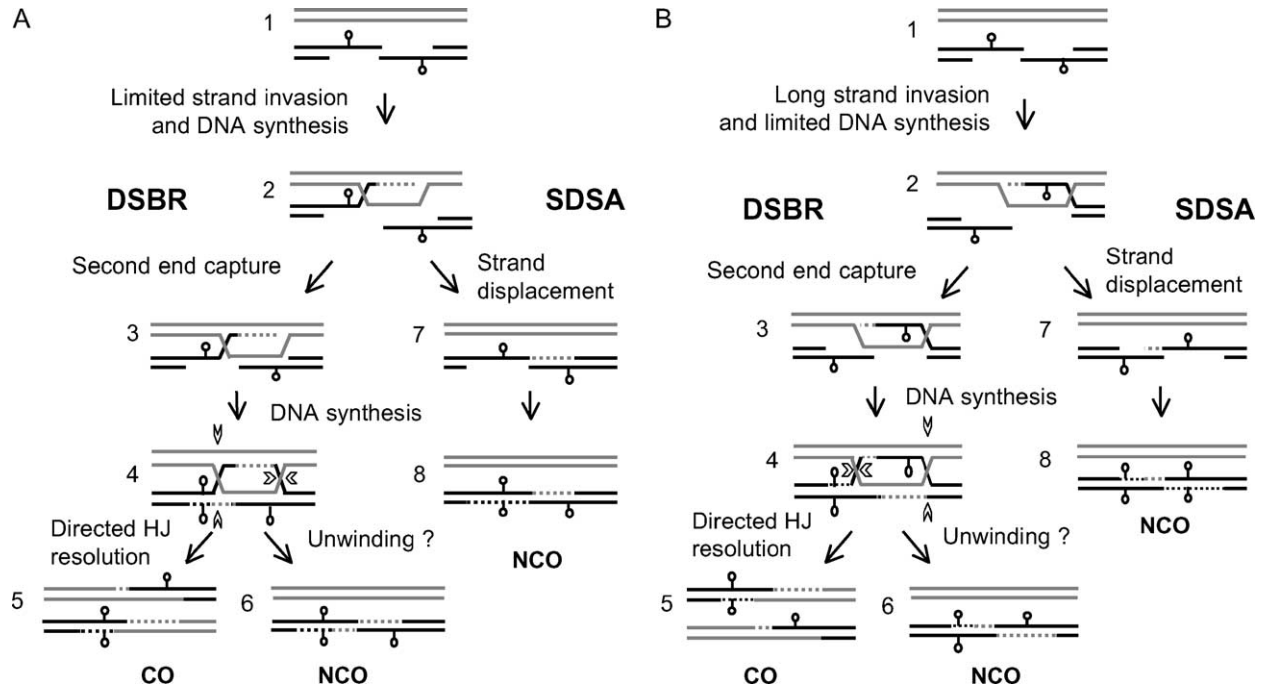

FIGURE 6.—Models for meiotic recombination based on our findings as well as those of others. (A) Extensive hDNA is formed by extension of the single-strand tail and second end capture. One end of the resected DSB invades homologous sequences forming a short (<300 bp) tract of hDNA and initiates DNA synthesis. NCO products arise through a SDSA pathway where the newly synthesized DNA is displaced and anneals to the other end of the DSB. A final round of DNA synthesis completes the mature NCO product. If the second end of the DSB is captured prior to strand displacement, a dHJ is formed. This intermediate is resolved by the two HJs in opposite directions (open arrowheads) to form CO products; only one of the two resolution modes is shown. A minor pathway for NCO production by unwinding the dHJ intermediate cannot be excluded. (B) Extensive hDNA is formed during initial strand invasion. One of the resected ends invades the homolog to form a tract of hDNA >600 bp. Capture of the second end of the resected DSB leads to formation of the dHJ that is resolved to form CO products as described above. Displacement of the newly synthesized strand in the intermediate shown in step 2 does not form an NCO gene conversion product.

sion is sometimes >140 bp, while our data indicate that invasion is most often <300 bp.

Relationship between DSB end resection and hDNA formation: 5′–3′ resection from the *ARG4* DSB is ~450 nt or more in two-thirds of broken chromosomes (SUN *et al.* 1991). At *HIS4*, DSBs are resected by ~600 nt (NAG and PETES 1993). We have also examined resection at the DSB site in our interval and find that the majority of breaks are resected >500 bp (data not shown). On the basis of these measures, most of the DSBs at the hotspot within the *URA3-ARG4* interval should be resected beyond *ura3-EcPal+104,* which is ~300 bp from the DSB. We expect that many are also resected beyond *arg4-EcPal+9*, 600 bp from the DSB. Tetrads with conversion of *arg4-EcPal+9* must have been produced by events where hDNA extended at least that distance. In the majority of such tetrads, *ura3-EcPal+104* is not converted. This indicates that, in single events where hDNA extends at least 600 bp from the initiating DSB in one direction, it rarely extends 300 bp in the other direction. Additional data consistent with short hDNA tracts are provided by the finding that many (~30% of ectopic and ~20% of allelic) crossovers map to the interval between the *ura3-EcPal+104* and *arg4-EcPal+9* palindromes, which contains the initiating DSB, without associated conversion of either marker. These findings support the suggestion that the average amount of hDNA formed during meiotic DSB repair is significantly less than the amount of single-strand DNA formed by resection, a conclusion also supported by electron-microscopy-based measurements of interjunction distances in dHJ intermediates (BELL and BYERS 1983). Below, we consider two ways in which this could occur, focusing on events in which *arg4-EcPal+9* is converted.

Initial strand invasion is short: Figure 6A presents a model in which the single-strand tail containing *ura3-EcPal+104* invades the homolog and initiates DNA synthesis that extends past the site of *arg4-EcPal+9*. Heteroduplex DNA will thus be present at *arg4-EcPal+9* in CO products and in NCO products, the latter irrespective of whether they are formed by SDSA (steps 7 and 8 in Figure 6A) or by the unwinding of a dHJ intermediate (step 6 in Figure 6A). For *ura3-EcPal+104* to be present in hDNA, at least in CO products, the initial strand invasion must be >300 bp. The frequent failure of this marker to be included in hDNA when *arg4-EcPal+9* is present in hDNA would indicate that initial strand invasion is <300 bp and thus less than the length of

resection. This conclusion—that the length of resection does not determine the length of strand invasion—was also reached by Merker *et al.* (2003).

Strand invasion is long: Figure 6B presents a model in which initial strand invasion is >600 bp and incorporates *arg4-EcPal+9* in hDNA. Parental segregation of *ura3-EcPal+104* would occur if the tract of DNA synthesis using the homolog as a template was <300 bp. This latter mechanism is consistent with the structure of the single end invasion (SEI) intermediates reported by Hunter and Kleckner (2001) in that the 3′-end of these three-arm intermediates does not show extensive DNA synthesis. Such intermediates could not produce NCO gene conversions of *arg4-EcPal+9* by an SDSA mechanism (steps 7 and 8 in Figure 6B), although these could still be produced by topoisomerase-mediated dHJ unwinding (step 6 in Figure 6B), as suggested by Gilbertson and Stahl (1996). Topoisomerase-mediated unwinding of dHJ intermediates would produce a single meiotic product with markers flanking the DSB site in a *trans* heteroduplex configuration (Figure 6A, step 6). Such bidirectional conversion products are detected, but only in a small minority of total conversion tetrads (Gilbertson and Stahl 1996; Merker *et al.* 2003; Hoffmann and Borts 2005; this study). Since the majority of the NCO events that we and others (Porter *et al.* 1993; Merker *et al.* 2003) observe appear to include only one marker in heteroduplex, our data do not address the likelihood of SDSA *vs.* dHJ unwinding. Arguments disfavoring dHJ unwinding as the predominant mechanism of NCO formation are provided by recent findings that both SEI and dHJ intermediates are on a crossover-predominant pathway (Hunter and Kleckner 2001; Börner *et al.* 2004) and that NCOs form at wild-type levels in mutants that fail to make either SEIs or dHJs (Börner *et al.* 2004) as well as in mutants that accumulate unresolved dHJs (Allers and Lichten 2001a; Clyne *et al.* 2003).

Modes of dHJ resolution: According to the DSBR model, COs are formed by dHJ resolution in which the two HJs are cut in opposite directions. Two possible CO-producing resolution modes are possible. In one (type 1 in Figure 5), strands ending 3′ at the original DSB (and their cognate strands on the other partner) are cut; in the other (type 2 in Figure 5), strands ending 5′ at the original DSB are cut, either near or within regions of newly synthesized DNA (dotted lines in Figure 5). Thus, the strands cut during formation of a crossover can be inferred from the position of the exchange point relative to the hDNA formed, and any bias in resolution will be revealed as an unequal recovery of the two types of crossovers. The modest bias that we observe toward type 2 resolution (Figure 5) is in the same direction as the bias inferred for recombination in both the *HIS4* and *ARG4* genes (Gilbertson and Stahl 1996; Foss *et al.* 1999; references within). Its molecular basis has not been identified, although it has been suggested that nicks or small gaps at the end of the tract of DNA synthesis might direct junction resolution (Foss *et al.* 1999). Such nicked or gapped structures (step 3 in Figure 6, A and B) have been proposed as a substrate for crossover formation by the Mus81/Mms4 nuclease (Osman *et al.* 2003; Hollingsworth and Brill 2004). However, this nuclease recognizes the free 5′-end at a flap junction or gap and nicks within the duplex five nucleotides upstream on the flap-containing strand (Bastin-Shanower *et al.* 2003). While this would resolve the DSB-distal junction (the HJ to the right of the palindrome in hDNA in Figure 5) in a manner consistent with our observations, we predict that the DSB-proximal junction (the HJ between the palindromes in Figure 5) would be much more than five nucleotides from the free 5′-end created by resection (which is at least 500 bp from the DSB; data not shown) and thus should not be a substrate for Mus81/Mms4 endonuclease cleavage. Furthermore, our observation of a substantial number of type 1 resolutions would indicate that nick-directed cutting cannot be the only mechanism for Holliday junction resolution.

We observed a few crossover tetrads where the point of exchange was separated from the marker showing PMS by an unconverted marker. The low frequency at which such crossovers are recovered among gene conversion tetrads (only slightly more than expected for two independent events) indicates that neither can be a major pathway for meiotic crossover formation at this locus. However, in a substantial fraction of crossover tetrads, neither marker displayed conversion and the point of exchange was separated from the DSB hotspot by an unconverted marker (in Table 3, 22% of ectopic crossovers and 33% of allelic crossovers, corresponding to 7% and 19% of total tetrads, respectively). There are several possible ways in which such crossovers, which we will term remote crossovers, might arise. Using *rad50S* strains, we did not detect enough DSBs at sites other than the *URA3-ARG4* DSB hotspot to account for the number of crossovers observed (see Figure 3 and supplemental Figure 1 at http://www.genetics.org/supplemental/). However, contributions from DSBs or other lesions not detected in *rad50S* mutants cannot formally be excluded. Alternatively, remote COs might arise from repair of DSBs formed at the *URA3-ARG4* hotspot accompanied by bubble migration, strand-displacement-mediated crossing over, or other mechanisms that move strand exchange structures away from an initiation site without creating intervening hDNA (Allers and Lichten 2001b; Smith 2001; Young *et al.* 2002). Such apparent remote COs can also be produced by the DSBR mechanism outlined in Figure 1, if dHJ resolution is directed toward type 1 resolution (Figure 5) and mismatches in hDNA are repaired to restore parental allele ratios (see Foss *et al.* 1999 for discussion); however, single remote crossovers are produced by this mechanism only if the hDNA formed is unidirectional or near-

unidirectional and does not include markers on both sides of the initiating DSB.

Conclusion: On the basis of our findings and those of others, we suggest the following mechanism for meiotic recombination in *S. cerevisiae* (Figure 6A). A 3′ single-strand tail from one end of the DSB invades homologous sequences and initiates DNA synthesis. This initial invasion is almost always <300 bp and frequently is <140 bp; on the other hand, extension of the tail can often extend >600 bp. The extended tail can be displaced and anneal with the other end of the resected DSB, yielding a NCO recombinant by SDSA; in such recombinants hDNA is present on only one side of the DSB (Figure 6, A or B). Double Holliday junction intermediates will be formed if the second end of the resected DSB is captured by the initial invasion intermediate (step 3 in Figure 6). By nature of the short initial invasion, very little hDNA is formed at the initial strand invasion step. The majority of hDNA is formed during second-strand capture. Resolution of the dHJ yields a CO product in which most of the hDNA is located to one side of the initiating DSB.

A second result of the short initial invasion is that one of the HJs in the dHJ intermediate will always be positioned close to the DSB, while the other HJ position will be dispersed. Unbiased resolution of these dHJ intermediates as COs (equal numbers of type 1 and type 2 resolution in Figure 5) will produce a population of products in which half contain exchange points near the DSB site, and half contain exchange points at dispersed locations. As a result, exchange points will appear to be concentrated near the DSB site. Biased junction resolution by preferentially cutting strands that contain newly synthesized DNA near the junction (type 2 resolution in Figure 5) will result in a further preferential location of the exchange point near the initiating DSB. Thus, one consequence of unidirectional or near-unidirectional hDNA formation will be a genetic map in which crossover distributions closely parallel those of DSBs (Wu and Lichten 1994) and crossover events appear to be highly localized, even when the resolution of that map is less than the average length of hDNA formed. Such highly punctuated crossover maps are typically seen at mammalian recombination hotspots (reviewed by Kauppi *et al.* 2004). Although short gene conversion tracts may contribute to this tight crossover localization, it also remains possible that it reflects an underlying unidirectionality in hDNA formation.

We thank Eva Hoffman and Rhona Borts for strains and for communicating results in advance of publication. We also thank Eva Hoffman, Rhona Borts, Tom Petes, Cyril Buhler, Robert Shroff, Gerry Smith, and three anonymous reviewers for discussions and comments that improved this manuscript.

LITERATURE CITED

Abdullah, M. F., and R. H. Borts, 2001 Meiotic recombination frequencies are affected by nutritional states in *Saccharomyces cerevisiae*. Proc. Natl. Acad. Sci. USA **98:** 14524–14529.

Alani, E., R. Padmore and N. Kleckner, 1990 Analysis of wild-type and *rad50* mutants of yeast suggests an intimate relationship between meiotic chromosome synapsis and recombination. Cell **61:** 419–436.

Allers, T., and M. Lichten, 2001a Differential timing and control of noncrossover and crossover recombination during meiosis. Cell **106:** 47–57.

Allers, T., and M. Lichten, 2001b Intermediates of yeast meiotic recombination contain heteroduplex DNA. Mol. Cell **8:** 225–231.

Bastin-Shanower, S. A., W. M. Fricke, J. R. Mullen and S. J. Brill, 2003 The mechanism of Mus81-Mms4 cleavage site selection distinguishes it from the homologous endonuclease Rad1-Rad10. Mol. Cell. Biol. **23:** 3487–3496.

Bell, L. R., and B. Byers, 1983 Homologous association of chromosomal DNA during yeast meiosis. Cold Spring Harbor Symp. Quant. Biol. **47** (Pt 2): 829–840.

Bergerat, A., B. de Massy, D. Gadelle, P. C. Varoutas, A. Nicolas *et al.*, 1997 An atypical topoisomerase II from Archaea with implications for meiotic recombination. Nature **386:** 414–417.

Borde, V., T.-C. Wu and M. Lichten, 1999 Use of a recombination reporter insert to define meiotic recombination domains on chromosome *III* of *Saccharomyces cerevisiae*. Mol. Cell. Biol. **19:** 4832–4842.

Börner, G. V., N. Kleckner and N. Hunter, 2004 Crossover/noncrossover differentiation, synaptonemal complex formation, and regulatory surveillance at the leptotene/zygotene transition of meiosis. Cell **117:** 29–45.

Borts, R. H., W. Y. Leung, W. Kramer, B. Kramer, M. Williamson *et al.*, 1990 Mismatch repair-induced meiotic recombination requires the *PMS1* gene product. Genetics **124:** 573–584.

Cao, L., E. Alani and N. Kleckner, 1990 A pathway for generation and processing of double-strand breaks during meiotic recombination in *S. cerevisiae*. Cell **61:** 1089–1101.

Cherry, J. M., C. Ball, S. Chervitz, K. Dolinski, S. Dwight *et al.*, 2002 *Saccharomyces* genome database (http://genome-www.stanford.edu/Saccharomyces/).

Clyne, R. K., V. L. Katis, L. Jessop, K. R. Benjamin, I. Herskowitz *et al.*, 2003 Polo-like kinase Cdc5 promotes chiasmata formation and cosegregation of sister centromeres at meiosis I. Nat. Cell Biol. **5:** 480–485.

Collins, I., and C. S. Newlon, 1994 Meiosis-specific formation of joint DNA molecules containing sequences from homologous chromosomes. Cell **76:** 65–75.

de Massy, B., V. Rocco and A. Nicolas, 1995 The nucleotide mapping of DNA double-strand breaks at the *CYS3* initiation site of meiotic recombination in *Saccharomyces cerevisiae*. EMBO J. **14:** 4589–4598.

Fan, Q. Q., F. Xu, M. A. White and T. D. Petes, 1997 Competition between adjacent meiotic recombination hotspots in the yeast *Saccharomyces cerevisiae*. Genetics **145:** 661–670.

Foss, H. M., K. J. Hillers and F. W. Stahl, 1999 The conversion gradient at *HIS4* of *Saccharomyces cerevisiae*. II. A role for mismatch repair directed by biased resolution of the recombinational intermediate. Genetics **153:** 573–583.

Gilbertson, L. A., and F. W. Stahl, 1996 A test of the double-strand break repair model for meiotic recombination in *Saccharomyces cerevisiae*. Genetics **144:** 27–41.

Goyon, C., and M. Lichten, 1993 Timing of molecular events in meiosis in *Saccharomyces cerevisiae*: stable heteroduplex DNA is formed late in meiotic prophase. Mol. Cell. Biol. **13:** 373–382.

Hoffmann, E. R., and R. H. Borts, 2005 *Trans* events associated with crossovers are revealed in *mlh1*Δ and *msh2*Δ strains in *Saccharomyces cerevisiae*. Genetics **169:** 1305–1310.

Hoffmann, E. R., E. Eriksson, B. J. Herbert and R. H. Borts, 2005 *MLH1* and *MSH2* promote the symmetry of double-strand break repair events at the *HIS4* hotspot in *Saccharomyces cerevisiae*. Genetics **169:** 1291–1303.

Hollingsworth, N. M., and S. J. Brill, 2004 The Mus81 solution to resolution: generating meiotic crossovers without Holliday junctions. Genes Dev. **18:** 117–125.

Hunter, N., and N. Kleckner, 2001 The single-end invasion: an asymmetric intermediate at the double-strand break to double-Holliday junction transition of meiotic recombination. Cell **106:** 59–70.

Kane, S. M., and R. Roth, 1974 Carbohydrate metabolism during ascospore development in yeast. J. Bacteriol. **118:** 8–14.

Kauppi, L., A. J. Jeffreys and S. Keeney, 2004 Where the crossovers

are: recombination distributions in mammals. Nat. Rev. Genet. **5:** 413–424.

Keeney, S., C. N. Giroux and N. Kleckner, 1997 Meiosis-specific DNA double-strand breaks are catalyzed by Spo11, a member of a widely conserved protein family. Cell **88:** 375–384.

Liu, J., T. C. Wu and M. Lichten, 1995 The location and structure of double-strand DNA breaks induced during yeast meiosis: evidence for a covalently linked DNA-protein intermediate. EMBO J. **14:** 4599–4608.

Merker, J. D., M. Dominska and T. D. Petes, 2003 Patterns of heteroduplex formation associated with the initiation of meiotic recombination in the yeast *Saccharomyces cerevisiae*. Genetics **165:** 47–63.

Nag, D. K., and T. D. Petes, 1993 Physical detection of heteroduplexes during meiotic recombination in the yeast *Saccharomyces cerevisiae*. Mol. Cell. Biol. **13:** 2324–2331.

Nag, D. K., M. A. White and T. D. Petes, 1989 Palindromic sequences in heteroduplex DNA inhibit mismatch repair in yeast. Nature **340:** 318–320.

Osman, F., J. Dixon, C. L. Doe and M. C. Whitby, 2003 Generating crossovers by resolution of nicked Holliday junctions: a role for Mus81-Eme1 in meiosis. Mol. Cell **12:** 761–774.

Paques, F., and J. E. Haber, 1999 Multiple pathways of recombination induced by double-strand breaks in *Saccharomyces cerevisiae*. Microbiol. Mol. Biol. Rev. **63:** 349–404.

Petes, T. D., R. E. Malone and L. S. Symington, 1991 Recombination in yeast, pp. 407–521 in *The Molecular and Cellular Biology of the Yeast Saccharomyces: Genome Dynamics, Protein Synthesis, and Energetics*, edited by J. Broach, E. Jones and J. Pringle. Cold Spring Harbor Laboratory Press, Cold Spring Harbor, NY.

Petronczki, M., M. F. Siomos and K. Nasmyth, 2003 Un ménage à quatre: the molecular biology of chromosome segregation in meiosis. Cell **112:** 423–440.

Porter, S. E., M. A. White and T. D. Petes, 1993 Genetic evidence that the meiotic recombination hotspot at the *HIS4* locus of *Saccharomyces cerevisiae* does not represent a site for a symmetrically processed double-strand break. Genetics **134:** 5–19.

Sambrook, J., and D. W. Russell, 2001 *Molecular Cloning: A Laboratory Manual*. Cold Spring Harbor Laboratory Press, Cold Spring Harbor, New York.

Schultes, N. P., and J. W. Szostak, 1990 Decreasing gradients of gene conversion on both sides of the initiation site for meiotic recombination at the *ARG4* locus in yeast. Genetics **126:** 813–822.

Schwacha, A., and N. Kleckner, 1994 Identification of joint molecules that form frequently between homologs but rarely between sister chromatids during yeast meiosis. Cell **76:** 51–63.

Smith, G. R., 2001 Homologous recombination near and far from DNA breaks: alternative roles and contrasting views. Annu. Rev. Genet. **35:** 243–274.

Sun, H., D. Treco, N. P. Schultes and J. W. Szostak, 1989 Double-strand breaks at an initiation site for meiotic gene conversion. Nature **338:** 87–90.

Sun, H., D. Treco and J. W. Szostak, 1991 Extensive 3′-overhanging, single-stranded DNA associated with the meiosis-specific double-strand breaks at the ARG4 recombination initiation site. Cell **64:** 1155–1161.

Szostak, J. W., T. L. Orr-Weaver, R. J. Rothstein and F. W. Stahl, 1983 The double-strand-break repair model for recombination. Cell **33:** 25–35.

Trueheart, J., J. D. Boeke and G. R. Fink, 1987 Two genes required for cell fusion during yeast conjugation: evidence for a pheromone-induced surface protein. Mol. Cell. Biol. **7:** 2316–2328.

White, M. A., M. Dominska and T. D. Petes, 1993 Transcription factors are required for the meiotic recombination hotspot at the *HIS4* locus in *Saccharomyces cerevisiae*. Proc. Natl. Acad. Sci. USA **90:** 6621–6625.

Wu, T.-C., and M. Lichten, 1994 Meiosis-induced double-strand break sites determined by yeast chromatin structure. Science **263:** 515–518.

Wu, T. C., and M. Lichten, 1995 Factors that affect the location and frequency of meiosis-induced double-strand breaks in *Saccharomyces cerevisiae*. Genetics **140:** 55–66.

Xu, F., and T. D. Petes, 1996 Fine-structure mapping of meiosis-specific double-strand DNA breaks at a recombination hotspot associated with an insertion of telomeric sequences upstream of the *HIS4* locus in yeast. Genetics **143:** 1115–1125.

Young, J. A., R. W. Schreckhise, W. W. Steiner and G. R. Smith, 2002 Meiotic recombination remote from prominent DNA break sites in *S. pombe*. Mol. Cell **9:** 253–263.

Communicating editor: G. Smith